Automatic Liver Segmentation Using a Statistical Shape Model With Optimal Surface Detection

Xing Zhang, Jie Tian*, *Fellow, IEEE*, Kexin Deng, Yongfang Wu, and Xiuli Li

***Abstract*—In this letter, we present an approach for automatic liver segmentation from computed tomography (CT) scans that is based on a statistical shape model (SSM) integrated with an optimal-surface-detection strategy. The proposed method is a hybrid method that combines three steps. First, we use localization of the average liver shape model in a test CT volume via 3-D generalized Hough transform. Second, we use subspace initialization of the SSM through intensity and gradient profile. Third, we deform the shape model to adapt to liver contour through an optimal-surface-detection approach based on graph theory. The proposed method is evaluated on MICCAI 2007 liver-segmentation challenge datasets. The experiment results demonstrate availability of the proposed method.**

***Index Terms*—Generalized Hough transform (GHT), liver segmentation, minimum *s–t* cut, principal component analysis (PCA), statistical shape model (SSM).**

I. Introduction

In THE area of computer-aided diagnosis (CAD), accurate and robust segmentation of liver tissue from medical images is a prerequisite for hepatic diseases diagnosis and surgery planning. Computed tomography (CT) volume is often used for liver segmentation and subsequent liver vasculature analysis. Due to the highly varying shape of liver and weak edge between some adjacent organs (e.g., heart, stomach, and muscles), liver segmentation becomes a challenging task that has attracted research attention recently. Specifically, MICCAI 2007 Workshop on 3-D liver segmentation (http://www.sliver07.org/) provides a platform for testing and comparing different approaches for the topic [1]. In the challenge, the statistical shape model (SSM) based method [2] has the best performance among all approaches.

The SSM-based segmentation framework was first proposed by Cootes *et al.* [3]. Techniques involved in the SSM include shape correspondence, shape representation, and search algorithms. In the shape-model construction process, establishing landmark points correspondence among all shapes of training sets is generally the most challenging step. Spherical harmonics (SPHARM) [4] mapping for each training shape is an effective registration method for shape correspondence, and the groupwise optimization strategy can produce better results than the pairwise method. Subsequently, a compact shape representation via classical principal component analysis (PCA) method can be applied for model construction. As the SSM-based approaches are sensitive to initialization (pose and shape parameters of the initial model), an initial position of the model should be estimated. In contrast with manual or the time-consuming evolutionary algorithm [5] proposed earlier, we present a 3-D generalized Hough transform (GHT) method to detect approximate location of the liver shape model. After the SSM adaption, the shape model is deformed to adapt to the liver contour through an optimal surface detection based on graph theory.

II. Hybrid Method for Liver Segmentation

A. Shape-Model Construction

The liver shape model is built from several ground truth segmentation results. After determining points correspondence for SSM and alignment of all training triangulated meshes based on similarity transform, the PCA is applied to represent variation modes of the training sets. Each valid liver shape vector can be approximated by the average shape vector plus a subspace spanned by the first c $(c \leq n)$ eigenmodes

$$\Phi \cong T^{-1}\left(\overline{\Phi} + \sum_{m=1}^{c} b_m p_m\right) \tag{1}$$

where $\overline{\Phi} = \sum_i \Phi_i / n$ is the average shape vector, p_m is the principal mode of variation obtained through PCA, b_m is the corresponding weight for each principal mode, and T is a similarity transform computed from the given shape Φ to the average shape $\overline{\Phi}$. An instance of an SSM should have a limitation of $b_m \in [-3\sqrt{\lambda_m}, 3\sqrt{\lambda_m}]$ for not producing large deviation from the training sets, where λ_m is the corresponding eigenvalue for each eigenvector p_m.

Manuscript received April 15, 2010; revised June 13, 2010; accepted June 24, 2010. Date of publication July 8, 2010; date of current version September 15, 2010. This work was supported by the National Basic Research Program of China under Grant 2006CB705700, by the Program for Changjiang Scholars and Innovation Research Team in University of Ministry of Education under Grant IRT0645, by the Hundred Talents Program of the Chinese Academy of Sciences by the Knowledge Innovation Program of the Chinese Academy of Sciences under Grant KSCX2-YW-R-262 and Grant KGCX2-YW-129, and by the Natural Science Foundation of China under Grant 30873462, Grant 60910006, Grant 30970769, and Grant 30970771. *Asterisk indicates corresponding author.*

X. Zhang, Y. Wu, and X. Li are with the Medical Image Processing Group, Institute of Automation, Chinese Academy of Sciences, Beijing 100190, China (e-mail: xing.zhang@ia.ac.cn; wuyongfang@fingerpass.net.cn; lixiuli@fingerpass.net.cn).

*J. Tian is with the Medical Image Processing Group, Institute of Automation, Chinese Academy of Sciences, Beijing 100190, China (e-mail: tian@ieee.org).

K. Deng is with the Life Science Research Center, Xidian University, Xi'an, Shanxi 710071, China (e-mail: dengkx@fingerpass.net.cn).

Color versions of one or more of the figures in this paper are available online at http://ieeexplore.ieee.org.

Digital Object Identifier 10.1109/TBME.2010.2056369

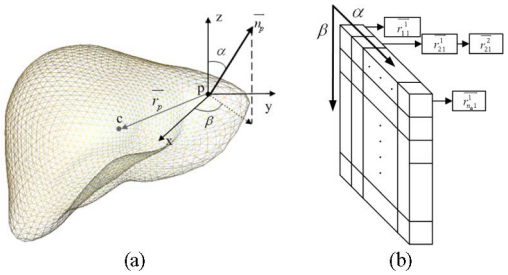

Fig. 1. Parameters involved in the 3-D GHT. (a) Revolution angle α and azimuthal angle β of the surface vertex normal is indexed as the entries of R-table. (b) Illustration of a 2-D R-table constructed by storing vector $\vec{r}$.

B. Liver Localization by 3-D GHT

Liver localization is a prerequisite for accurate liver segmentation. Hough transform is an effective and robust method to detect any arbitrary shape in an image [6]. During GHT learning process, the triangulated mesh of the average shape model is employed as a template shape. As shown in Fig. 1, the liver centroid *c* is used as the reference point. For each vertex *p* on the surface, revolution angle α and azimuthal angle β of the vertex normal $\overrightarrow{n_p}$ are discretized as the entries of the 2-D reference table (R-table). The R-table constructed by storing vector $\overrightarrow{r_p}$ for each vertex *p* is indexed by α and β, as shown in Fig. 1(b). When detecting liver shape in a test volume, the gradient angle α and β of an edge point is employed to retrieve corresponding entries of the R-table. An accumulator array for parameter space saves the votes of edge points to determine the most probable center of liver.

In order to reduce dimensionalities of the parameter space, we only restrict the average shape model transform under translation and isotropic scaling that neglects rotation. The transformation requires a 4-D parameter space storage. The experiments show that the assumption can effectively reduce computational cost while giving acceptable localization result. For an edge point $\overrightarrow{v_q}$ in a test image, the corresponding $\overrightarrow{r_q}$ can be determined by gradient direction of the edge point. Then, the possible location of reference point in the parameter space is calculated from $\overrightarrow{v_q} + s\overrightarrow{r_q}$, where *s* denotes the scaling factor.

Before liver localization, the CT volume requires preprocessing.

1) *Image downsampling:* Three-dimensional GHT is performed on low-resolution layer of the CT volume to capture global information while improving efficiency. The original CT volume is downsampled to $3 \times 3 \times 3$ mm^3 using linear interpolation. Since the scale of the liver is more larger than the spacial sampling interval, the shape of liver can be preserved well after downsampling process.
2) *Image smoothing:* In order to eliminate staircase edges that resulted from downsampling, a mean filter is employed to smoothen the downsampled CT volume.
3) *Edge detection:* The edges of the volume is detected through Canny edge detector while pruning edges that definitely do not belong to the liver boundary. The liver has a CT value range of $[I_{\text{low}}, I_{\text{high}}]$, edges with corresponding CT value out of the range will be pruned for an accurate and fast GHT localization.

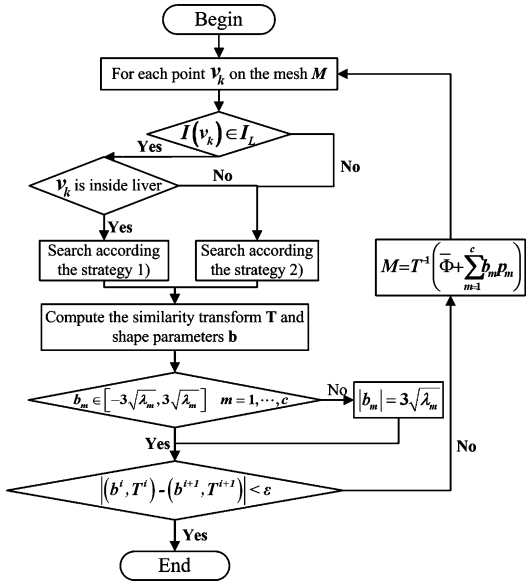

Fig. 2. Flowchart of the subspace initialization step.

C. Subspace Initialization of the SSM

Previous to the subspace initialization step, a 3-D nonlinear diffusion filter is applied to a test volume for reducing noise while preserving liver contour. The nonlinear diffusion equation is given as follows:

$$\begin{cases} \dfrac{\partial u(x,y,z,t)}{\partial t} = div[g(|\nabla u|^2)\nabla u] \\ u(x,y,z,0) = u_0(x,y,z) \end{cases} \tag{2}$$

where the diffusivity function $g(s) = 1 - \exp(-3.315(\lambda/s)^4)$, if $s > 0$ and $g(s) = 1$ otherwise.

An instance of the SSM demands computing a similarity transformation *T* and shape parameters b_m in (1). Designing an appropriate search strategy is very crucial. The flowchart is shown as Fig. 2. Suppose the CT value range of liver is $I_L = [I_{\text{low}}, I_{\text{high}}]$, and $g_{\max}$ denotes the maximum gradient magnitude of the liver boundary. For each vertex $\overrightarrow{v_i}$ on the mesh, candidate liver boundary point is searched along the vertex normal $\overrightarrow{n_i}$, *N* equidistant points are sampled along each vertex normal direction: $\overrightarrow{v_k} = \overrightarrow{v_i} + (k - (N-1)/2) \bullet d \bullet \overrightarrow{n_i}$ $(k = 0, \ldots, N-1)$, where *d* is the sampling distance. For an initial vertex v_k $(k = (N-1)/2)$ on the mesh, if $I(v_k) \in I_L$, then count the number *c* of consecutive $i \le k$ with $I(v_i) \in I_L$, the vertex v_k is considered inside the liver when $c \ge c_{\text{thresh}}$, otherwise v_k is outside the liver. Based on these assumptions, two different strategies are used for searching candidate points, which are as follows.

1) v_k *is inside the liver:* search candidate points from $i = (N-1)/2$ with $i \in [\frac{N-1}{2}, N-1]$, count number *c* of consecutive points $I(v_i) \in I_L$ and $|\nabla I(v_i)| \le g_{\max}$, set $k = (N-1)/2 + c$.

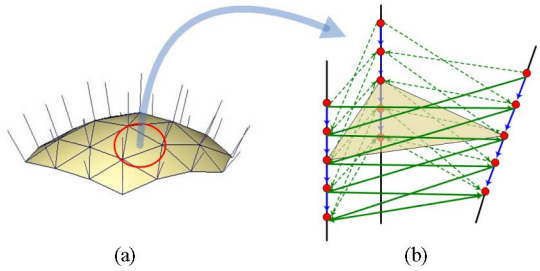

Fig. 3. Graph construction. (a) Triangulated surface mesh with vertex normals. (b) Graph is constructed with intracolumn arcs and intercolumn arcs. The blue edges denotes the intracolumn arcs, while green edges denotes the intercolumn arcs. Smoothness constraint in this graph is $\Delta = 1$.

2) v_k *is outside the liver:* search candidate points from $i = 0$ with $i \in [0, \frac{N-1}{2}]$, count number c of consecutive points $I(v_i) \in I_L$ and $|\nabla I(v_k)| \leq g_{\max}$, set $k = c$.

D. Optimal-Surface-Detection Approach Based on Graph Theory

The segmentation result of the subspace initialization is just a linear combination of variation modes described in (1), which abundantly exploits prior typical liver shape, but it lacks flexibility to adapt to a liver in an arbitrary test volume. Based on the previous segmentation result, we employ an optimal-surface-detection algorithm proposed by Li *et al.* [7] in the final refined segmentation process. The algorithm can globally optimize a cost function that incorporates sum of nodes cost and surface smoothness constraint by transforming it to a minimum *s–t* cut problem.

The graph is constructed in a narrowband around the segmented surface. Suppose a vertex $\overrightarrow{v_i}$ on the mesh and its normal $\overrightarrow{n_i}$, N equidistant points are sampled along each vertex normal direction for composing a column: $\overrightarrow{p_k} = \overrightarrow{v_i} + (k - (N-1)/2) \bullet d \bullet \overrightarrow{n_i}$ $(k = 0, \ldots, N-1)$. As shown in Fig. 3(b), there are two types of arcs in the graph, intracolumn arcs and intercolumn arcs. For each column in the graph, the intracolumn arcs is $E^a = \{\langle p_k, p_{k-1}\rangle | k = 1, \ldots, N-1\}$, the blue edges shown in Fig. 3(b) denote the intracolumn arcs.

The intercolumn arcs express the smoothness constraint. Consider two neighboring columns P_m and P_n in the graph, the intercolumn is $E^r = \{\langle p_k^m, p^n_{\max(0,k-\Delta)}\rangle | \forall P_m, P_n$ is adjacent$\}$, where the smoothness constraint Δ represents the maximum-allowed difference between two neighboring points on a surface. The green edges shown in Fig. 3(b) denote the intercolumn arcs.

Both the intracolumn and intercolumn arcs are regarded as *n* links in a graph and assign infinity. In the weighted directed graph, each node has a weight $w(v_k)$. Nodes with $w(v_k) \geq 0$ are connected to the sink terminal by a directed edge of weight $w(v_k)$, while nodes with $w(v_k) < 0$ are connected to the source terminal by a directed edge of weight $-w(v_k)$. The weight w_k^m of *k*th point in the *m*th column is defined as (3). The cost function *c* used in (3) is negative gradient magnitude $c(v_k) = -|\nabla I(v_k)|$ if v_k lies inside or on the boundary of the liver and $c(v_k) = 1$ otherwise. Whether a sample point is inside or outside the liver can be determined using the same rule as in the subspace initialization step. The negative gradient magnitude $-|\nabla I(v_k)|$ is computed in image domain, and then, the node cost is derived by linear interpolation according to the coordinate of the node.

$$w_k^m = \begin{cases} c_k^m, & k = 0 \\ c_k^m - c_{k-1}^m, & \text{otherwise.} \end{cases} \tag{3}$$

TABLE I
PARAMETERS SELECTION

Step	Parameters
1. 3D GHT	$\Delta\alpha = \frac{\pi}{20}$, $\Delta\beta = \frac{\pi}{20}$, scaling factor $s \in [0.9, 1.0, 1.1]$, $[I_{low}, I_{high}] = [50, 200]$
2. Nonlinear diffusion	$\lambda = 800$, $\Delta t = 0.15$, t = 1.5
3. Subspace initialization	sampling distance d=1 mm, sampling points N = 41, $g_{\max} = 200$, $c_{\text{thresh}} = 10$, $\varepsilon = 2$, all 40 variation modes are used
4. Optimal surface detection	sampling distance d =1 mm, sampling points N = 31, smoothness constraint $\Delta = 2$

III. EXPERIMENTS AND RESULTS

The proposed method is tested on the training and testing datasets of MICCAI 2007 liver-segmentation challenge. There are 20 CT volumes of abdomen with contrast agent in the training datasets, and ten in the testing datasets. All datasets have an in-plane resolution of 512×512 pixels and interslice spacing from 0.5 to 5.0 mm. Other 40 CT volumes with normal liver anatomy obtained clinically are used for shape-model construction with 2562 equally distributed vertices and 5120 triangles on each model. Points correspondence for SSM was established via an open-source software developed by Heimann *et al.* [8]. We implemented our method based on the medical imaging toolkit (MITK http://www.mitk.net/) developed by our group on a 32-bit desktop PC (2.33 GHz Core 2 and 2 GB RAM).

A. Segmentation Workflow and Parameters Selection

The segmentation workflow consists of following steps:
1) average shape-model localization through 3D GHT;
2) nonlinear diffusion filtering;
3) model subspace initialization;
4) refined segmentation based on optimal surface detection.

The parameters for each step are listed in Table I.

B. Results

The average run time for each step of ten testing datasets in liver localization is given in Table II. Due to performing in the subsampled volume, the edge detection and 3-D GHT process step just takes about 2 s, respectively. The average whole processing time of localization is about 4.47 s in comparison to 6 min by the evolution method [5]. Since it proceeds iteratively with six parameter space, the previously proposed evolution method is time consuming. Fig. 4 shows the result of each preprocessing step in liver localization. Downsampling is used to capture the global shape of the liver while reducing computational time. GHT needs to perform on a binary edge

TABLE II
AVERAGE RUN TIME OF EACH STEP IN LIVER LOCALIZATION

Process step	Downsample	Smooth	Edge detect	3D GHT
Run time (seconds)	0.13	0.14	2.07	2.13

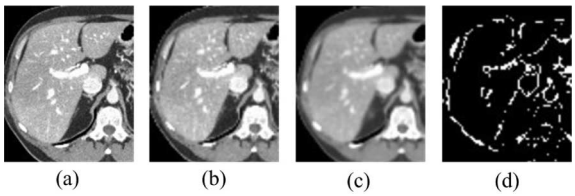

Fig. 4. Preprocessing steps of the 3-D GHT. (a) Original image. (b) Downsampled image. (c) Smoothed image. (d) Canny edge detection.

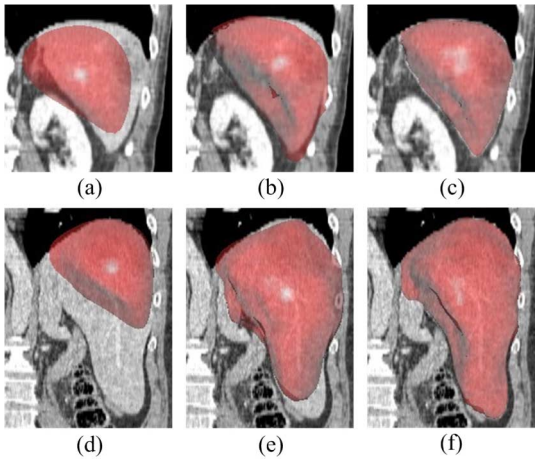

Fig. 5. State of the surface mesh in a coronal slice from back after each segmentation step. The top row shows a relatively easy case (testing data 5) while the bottom row shows a relatively difficult case (testing data 4). (a) and (d) After localization by 3-D GHT. (b) and (e) After model subspace initialization. (c) and (f) Final result after optimal surface detection.

image. However, the initial downsampling step will bring on staircase edges that cause discrete orientations on edge points. A smoothing filter is necessary for eliminating the staircase edges effect.

State of the surface mesh after each segmentation step is illustrated in Fig. 5. Fig. 5(top) shows a liver that is similar to the average shape, while Fig. 5(bottom) shows a liver with long lobus hepatis dexter that has a large deviation from the average shape. As shown in Fig. 5, after an initial location is given by 3-D GHT, an instance of SSM is adapted to the liver. Finally, the accurate contour of liver is detected through the optimal graph-search strategy. The SSM initialization process takes about 2.86 min, while the optimal surface detection takes about 8 s.

The resulting surface meshes are converted to volume with the same dimension and spacing as the corresponding CT volume datasets. Fig. 6(a) shows a surface distance map from the segmentation result to the reference result of a training dataset. Segmentation results are compared to the reference results according to the following five metrics: volumetric overlap error (OE), signed relative volume difference (SVD), symmetric average surface distance (D_{Avg}), symmetric rms surface distance (D_{rms}), and maximum surface distance (D_{Max}). The five average-segmentation-results metrics of 20 training datasets achieved by the proposed method are summarized in Table III in comparison with previous works from literature. OE and D_{Avg} are the most comprehensive metrics of segmentation error among the previous five. Our approach results in low segmentation error in respect to metric OE (5.25%) and D_{Avg} (0.93 mm). However, it achieves a relatively high D_{Max} (24.80 mm). In some cases, the triangulated mesh after subspace initialization is locally sparse in some long and narrow regions (e.g., left lateral lobe and right posterior lobe) of liver; therefore, it will cause large D_{Max}, as shown in Fig. 6(b).

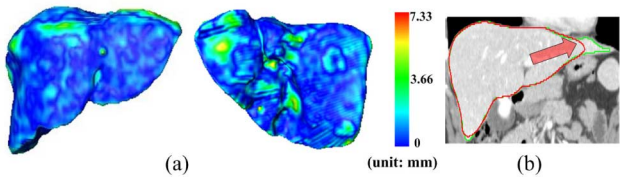

Fig. 6. (a) Surface distance map from the segmentation result to the reference result of a training dataset. (b) Segmentation error in the sharp of left lateral lobe. The contour of the reference result is in green, while the contour of the segmentation result is in red.

TABLE III
RESULTS OF COMPARISON METRICS WITH PREVIOUS WORKS

Method	OE [%]	SVD [%]	D_{Avg} [mm]	D_{RMS} [mm]	D_{Max} [mm]
Kainmueller[2]	6.96	-3.57	1.10	2.25	20.95
Heimann[5]	5.1	n/a	1.6	3.3	n/a
Lamecker[9]	7.0	n/a	2.3	3.1	n/a
Our approach	5.25	0.73	0.93	2.23	24.80

IV. CONCLUSION AND FUTURE WORKS

The letter presents a hybrid method based on an SSM to perform automatic liver segmentation from CT scans. The experiments demonstrate effectiveness of the proposed method. Segmentation errors may occur at some long and narrow regions of liver. In order to reduce deviation, more landmark points on each model will be employed in shape-model construction.

Though 3-D GHT provides acceptable liver localization of the average shape model just under translation and isotropic scaling, the major drawback of GHT is that the scale and rotation of the object are handled in a brute-force manner that requires a 6-D parameter space and high computational cost. An orientation and scale-invariant GHT method may solve the problem. In the subspace initialization step, the candidate points searching process proceeds iteratively and takes most of the time, but it is suitable to be parallelized for acceleration. In the final optimal-surface-detection step, graph nodes are sampled in all columns with the same sampling distance. In future works, each vertex-column sampling distance depends on sparsity of the local triangulated mesh for improving accuracy.

REFERENCES

[1] T. Heimann, B. van Ginneken, M. Styner, Y. Arzhaeva, V. Aurich, C. Bauer, A. Beck, C. Becker, R. Beichel, G. Bekes, F. Bello, G. Binnig, H. Bischof, A. Bornik, M. M. Cashman, Y. Chi, A. Cordova, M. Dawant, M. Fidrich, D. Furst, D. Furukawa, L. Grenacher, J. Hornegger, D. Kainmuller, I. Kitney, H. Kobatake, H. Lamecker, T. Lange, J. Lee, B. Lennon, R. Li, S. Li, H. Meinzer, G. Nemeth, S. Raicu, A. Rau, M. van Rikxoort, M. Rousson, L. Rusko, A. Saddi, G. Schmidt, D. Seghers, A. Shimizu, P. Slagmolen, E. Sorantin, G. Soza, R. Susomboon, M. Waite, A. Wimmer, and I. Wolf, "Comparison and evaluation of methods for liver segmentation from CT Datasets," *IEEE Trans. Med. Imag.*, vol. 28, no. 8, pp. 1251–1265, Aug. 2009.

[2] D. Kainmueller, T. Lange, and H. Lamecker, "Shape constrained automatic segmentation of the liver based on a heuristic intensity model," in *Proc. MICCAI Workshop 3-D Segmentation Clin.: Grand Challenge*, 2007, pp.109–116.

[3] T.-F. Cootes, C.-J. Taylor, D.-H. Cooper, and J. Graham, "Active shape models—Their training and application," *Comput. Vis. Image Underst.*, vol. 61, no. 1, pp. 38–59, Jan. 1995.

[4] A. Kelemen, G. Szekely, and G. Gerig, "Elastic model-based segmentation of 3-d neuroradiological data sets," *IEEE Trans. Med. Imag.*, vol. 18, no. 10, pp. 828–839, Oct. 1999.

[5] T. Heimann, S. Munzing, H.-P. Meinzer, and I. Wolf, "A shape-guided deformable model with evolutionary algorithm initialization for 3D soft tissue segmentation," in *Proc. IPMI* (Lecture Notes Comput. Sci.), vol. 4584. New York: Springer-Verlag, 2007, pp. 1–12.

[6] K. Khoshelham, "Extending generalized hough transform to detect 3d objects in laser range data," in *Proc. ISPRS Workshop Laser Scanning*, Espoo, Finland, 2007, pp.206–210.

[7] K. Li, X. Wu, D.-Z. Chen, and M. Sonka, "Optimal surface segmentation in volumetric images—A graph-theoretic approach," *IEEE Trans. Pattern Anal. Mach. Intell.*, vol. 28, no. 1, pp. 119–134, Jan. 2006.

[8] T. Heimann, I. Oguz, I. Wolf, M. Styner, and H.-P. Meinzer, "Implementing the automatic generation of 3d statistical shape models with ITK," in *Proc. MICCAI Open Sci. Workshop*, Copenhagen, Denmark, 2006, pp. 1–22.

[9] H. Lamecker, T. Lange, and M. Seebaee, "Segmentation of the liver using a 3d statistical shape model," Zuse Institute, Berlin, ZIB Tech. Rep., pp. 1–25, 2004.